

Preliminary Results of 7-Channel Insertional pTx Array Coil for 3T MRI

Yeun Chul Ryu*

Department of Radiological Science, Gachon University, Incheon 21936, Republic of Korea

(Received 10 April 2017, Received in final form 8 May 2017, Accepted 11 May 2017)

In this research, we report the preliminary results of an insertional type parallel transmission (pTx) array that has 7-elements that are placed in the space above a patient table as a transmit (Tx) coil to give an RF transmission (B_1^+) field for the body object of a 3 Tesla (T) MRI system. In previous research, we have tried to compare the performances of different coil elements and array geometries for a pTx body image. Based on these results, we attempt to obtain a human image with the proposed pTx array. Through the simulation and experimental results, we introduce a possible structure of multi-channel Tx array and verify the utility of a multi-channel Tx body image using B_1^+ shimming. The insertional pTx array, combined with a receiver (Rx) array coil, provides an enhanced B_1^+ field homogeneity in a large ROI image as a result of B_1^+ shimming applied over the full body size object. Through this research, we hope to determine the usefulness of the proposed insertional type RF coil combination for 3 T body imaging.

Keywords : parallel transmission, shimming, 7-channel transmission array, B_1^+ field, 3 Tesla

1. Introduction

An increased magnetic field strength improves the signal intensity and signal-to-noise ratio (SNR) of Magnetic Resonance Imaging (MRI). Recent development trends in MRI systems have been focused on handling the characteristics of high-field (HF) or ultra-high-field (UHF) electromagnetic waves. However, owing to the higher dielectric constant of human internal organs compared to air, the penetrating RF signal wavelength is shorter than that in a free space. The shortened wavelength produces a complicated inhomogeneous magnetic field penetration in the human body resulting in deterioration of MR images. The inhomogeneity of a magnetic field is highly affected by the operating frequency, the region of interest (ROI), and the complexity of the object's internal structures [1, 2].

As one prominent method for obtaining high-quality images in UHF MRI, the parallel transmission (pTx) technique has been verified in many studies by improving the homogeneity of the transmitted field. The pTx technique is a multi-channel simultaneous transmission method that adjusts the RF field to a desired pattern [3-5]. Multi-channel radio frequency (RF) coils that can indepen-

dently and simultaneously transmit RF signals take advantage of the pTx method. In the case of 3 Tesla (3 T) commercial systems, the most generalized type of body transmit RF coil is the 2-channel birdcage-type quadrature body coil. However, the usage of the birdcage coil in pTx mode, with its limited number of channels, is bounded by insufficient freedom of RF transmit operation. For this reason, it is difficult to completely resolve the magnetic field inhomogeneity issue in a higher magnetic field. In previous studies on the required degree of freedom for a 3T body image in pTx operation, it was suggested that the 4-channel degree of freedom with four variables and 3T body RF transmission (B_1^+) shimming would be sufficiently conducted, only with the degrees of freedom based on eight independent channels that have amplitude and phase as variables [6]. Currently, some research groups are attempting to replace the existing body transmit RF systems with pTx systems for the RF transmission method for a UHF body image. However, the replacement of the entire RF system for pTx is commonly restricted by the limitations of time and cost.

In recent studies on pTx RF coils for 3 T and 7 T MRI, multichannel transmit RF coils were added onto the RF system to realize the pTx method. These additional Tx array coils were installed in the inner space between the patient and RF coil frame to provide the pTx transmission array with the ability to be operated without the need to

©The Korean Magnetism Society. All rights reserved.

*Corresponding author: Tel: +82-32-820-4410

Fax: +82-32-460-8230, e-mail: yeunchul.ryu@gachon.ac.kr

replace the existing body coils [7]. However, there are some unsolved coil-design issues when using the additional coil method for 3 T pTx arrays. The first issue is the requirement of a novel power-efficient coil element design, because the RF field properties at 3 T are different from those of 7 T. Second, some transmit (Tx) coil elements, which act as the Tx power source, are attached to or very close to the human body; this will generate a high SAR distribution over the patient. This, in turn, creates an issue in high-powered applications such as turbo-spin echo pulse sequence. In addition, since the signal is vulnerable to body movements such as breathing, the transmit coil attached to the patient's body may suffer from motion artifacts and deterioration in image quality from unexpected feeding of the RF field.

In the previous studies performed by our group [8, 9], an insertional pTx array structure with field efficient Transverse electromagnetic (TEM) elements was suggested as a method to realize the pTx operation in existing commercial 3 T MRI systems by simulation. In this research, we report the implemented 7-channel pTx array of an insertional structure and show its utility through simulation and MRI experiments. The proposed 3 T pTx array designs are used for magnetic field homogeneity analysis on the B_1^+ field, and the implemented array is used for human imaging to compare to the results of a simulation.

2. Methods and Experiments

As reported in the previous research [8], the insertional upper-type pTx array shows good uniformity and power transfer efficiency compared to cylindrically structured birdcage coils or equi-angle and -distance positioned 8-channel TEM arrays. In this research, we implement an equi-angle 7-channel transmit array for body imaging. The element's design and location used in the 7-channel transmit array are very similar to those in the upper array part of the upper-lower coil structure shown in the previous research. Compared to the previous study, we do not implement the single channel, which is positioned above the patient, because of the reduction of the risk of electrical shorting caused by the patient's weight. Since the elements forming the array are mainly located in the upper area of the space between the patient table and the cylindrical RF coil frame, the array coil can be formed as a single frame. In addition, it can be easily installed and can provide a relatively homogeneous magnetic field in the upper space of the patient table. To compare the magnetic field properties of pTx array structure under different driving modes (e.g., quadrature driving and

optimized driving), the modeling for the simulation and methods for image acquisition have been designed as follows.

2.1. The design of 7-channel insertional frame-type pTx array and its coil elements

The structures of the TEM elements used for the pTx array formation are shown in Fig. 1. The TEM elements comprised two copper plates and tuning capacitors. The upper plate for the main field generation had a 1-cm wide and 42-cm long conducting wire. The lower plate for the RF shield and the returning path had a 3.5-cm wide and 50-cm long conducting plate. Both plates were spaced 2.5 cm apart. The TEM elements had an identical geometry and capacitance values in all the arrays. All the specifications used for the array structure were based on the open information of a Tim trio 3 T MRI system (Erlangen, Germany) that was modified to have 8-channel parallel transmission capability.

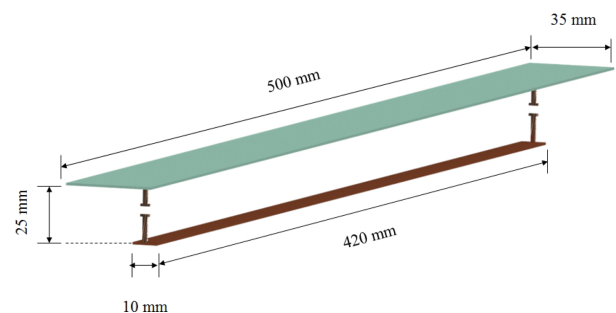


Fig. 1. (Color online) A strip-line type TEM element used for the pTx array. Green plates provide the return path acting as the RF ground and the brown plates generate the RF.

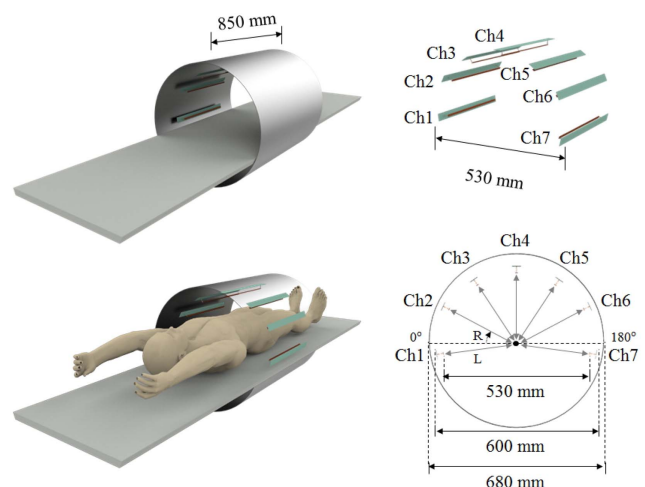


Fig. 2. (Color online) The structure of the upper insertional 7-channel pTx array. The elements are placed at equi-angle locations between the patient body and the existing body coil frame. All the elements are designed identically.

Table 1. The distance and geometric angles of each coil element. The reference point was set to the magnet’s isocenter. The channel number and location are shown in Fig. 2. The angle is expressed within the range 0° to 360° .

	Ch1	Ch2	Ch3	Ch4	Ch5	Ch6	Ch7
L [mm]	225	225	200	200	200	225	225
R [$^\circ$]	355	25	55	90	125	155	190

The upper insertional frame type pTx array design used in this research is shown in Fig. 2 and each element position is shown in Table 1. The upper insertional frame type pTx array coils were arranged in the upper area of the inner bore of the existing body coil frame. All the elements were arranged inside the 60 cm diameter RF coil frame at an equi-angle from the isocenter of the magnet. However, the 3-channel elements located in the uppermost area were arranged 3 cm lower than the other elements in order to improve the weak magnetic field in the lower area of the human body. In this manner, we can enhance the B_1^+ field on the back side of the patient, which is the farthest area in the region of interest (ROI), and we can also minimize the interference effects caused by the existing body coil when the insertional coil was installed. The homemade upper frame was implemented with 7-channel transmit array coil elements and is shown in Fig. 3. Each of the coil elements were connected to matching circuits and a ground breaker. The coaxial cable from the elements to the T/R switch box was equipped at every quarter lambda with cable traps for breaking RF-induced shield currents. The RF power supplied to each channel of the pTx array is provided by an independent 8-

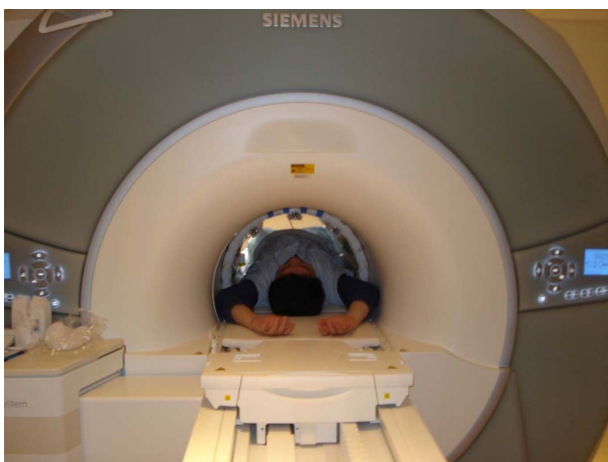


Fig. 3. (Color online) The implemented insertional frame type 7-channel pTx array coil with a patient. The 7 TEM elements were located in the upper area of the patient within the inner bore of the existing body coil frame.

channel power amplifier (ANALOGIC, USA).

2.2. RF field simulation and human image

Simulations for investigating the pTx array coil properties were conducted using xFDTD software (REMCOM, USA). The resonance frequency was set at 123 MHz, which was the operating frequency of the 3 T MRI. To confirm the B_1^+ field of the multichannel transmit coil, the B_1^+ field of each element was calculated individually. The result was recalculated through the prepared MATLAB (MathWorks, USA) program for combining fields. The B_1^+ field had a transverse magnetization vector value in the rotating frame around the z-axis at 123 MHz. The mesh was designed with dimensions $180 \times 80 \times 448$ in the directions of x, y and z, respectively, and each cell size was $5 \times 5 \times 5 \text{ mm}^3$. The male human model, Duke (IT’IS, Switzerland), was used to investigate the electromagnetic properties of the human body with a resolution of $5 \times 5 \times 5 \text{ mm}^3$, which is the same as that of the unit cell. The pose of the human model was changed to the upper arm pose and transformed to an adequate form to enable finite-difference time-domain (FDTD) processing. The center of the multichannel transmit coil was positioned at the abdomen of the human model. The homogeneity was calculated using the axial 2D plane, including the center point of the ROI. The coil elements were modeled including two current-driving sources between the conducting and ground plates. Unlike the case of the voltage source method, no feeding board for tuning and matching was required. No decoupling circuit was used to offset the interference from nearby elements in order to simplify the structure. A geometric phase of elements was added on the driving source of each element for the circular quadrature driving mode.

To investigate the shimmed (or optimized) transmit RF field, the B_1^+ fields of each channel were fed to B_1^+ shimming program (NYU, USA) [10], the homogeneity levels of the reformed magnetic fields were then compared. The channel field map was processed using a homemade MATLAB program from the results for the field values of the xFDTD simulation. Statistics were calculated only taking into account the field of the human body using a mask. B_1^+ Shimming, which determines the magnetic field uniformity, was conducted using the MATLAB GUI program.

The B_1^+ shimmed field data were investigated through acquisition of a flip angle map. The actual field over the human object was acquired with the AFI (Actual Flip-angle) method [11]. The resultant human image optimized B_1^+ shimming was performed with a gradient echo image on the prostate. The imaging of the human body was

performed in the Tim trio 3T MRI system of Siemens, Germany.

3. Results and Discussions

3.1. Implementation of 7-channel pTx array

The 7-channel pTx array was implemented for the 3 T MRI system. The frame was manufactured with a laser-cutting machine and assembled with plastic material. The frame was a close fit to the inner bore of the existing body coil frame, which has a diameter of 60 cm. Between the conductor and ground plates, a machined wood pole was used for forming the distance between the two plates. Matching and tuning circuits were implemented in the coil element. All the coil elements were tuned to 123 MHz and the isolation between neighboring elements was measured with a network analyzer. The worst isolation was -11 dB and the tuning range was -16 dB to -23 dB. The implemented pTx array is shown in Fig. 3. Each coil element was fed with individual driving RF power amplifiers.

3.2. B_1^+ field calculation and shimming

The B_1^+ field map of each Tx channel was calculated from the xFDTD simulation. After the shimming process was performed, the optimal driving amplitude and phase were recorded and are shown in Table 2. In the shimming process, the maximum B_1^+ field uniformity in the com-

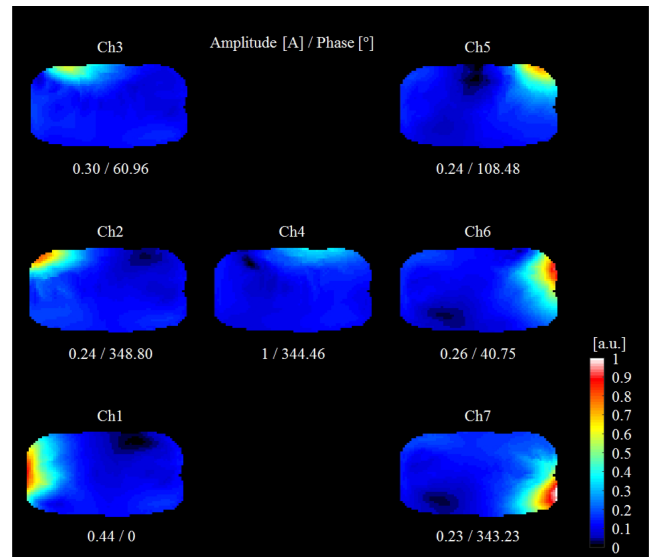


Fig. 4. (Color online) The optimized channel driving parameters and B_1^+ map of each channel for B_1^+ shimming over the male phantom data. The unit used in this figure is a relative value to the maximum value over all B_1^+ values in the axial center slice.

posite field was prioritized. The amplitude values are given relative to the maximum current channel (channel 4) and the phase values are given relative to the phase of channel 1. The data for the optimized channel driving parameters and B_1^+ map of each channel for the B_1^+

Table 2. The optimized parameters of each channel for B_1^+ shimming. The amplitude values are given relative to the maximum current channel (channel 4) and the phase values are given relative to the phase of channel 1 in units of degrees.

	Ch1	Ch2	Ch3	Ch4	Ch5	Ch6	Ch7
Amplitude [A]	0.44	0.24	0.30	1	0.24	0.26	0.23
Phase [°]	0	348.80	60.96	344.46	108.48	40.75	343.23

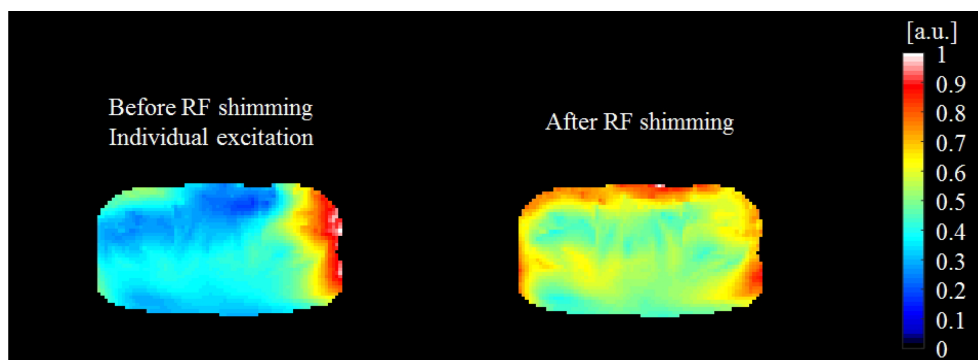


Fig. 5. (Color online) The effects of B_1^+ shimming in the simultaneous operation of every channel. Left is B_1^+ map before shimming and right is the B_1^+ map after shimming. In the right image, all the Tx channels were modified with an optimized amplitude and phase numbers from the B_1^+ shimming program.

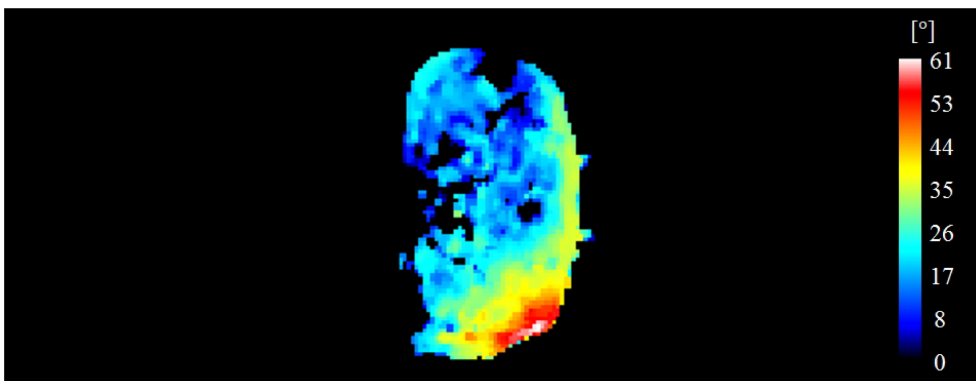


Fig. 6. (Color online) A flip angle map from the AFI method over the actual human body. The Tx array was operated in the shimmed circular driving mode with the optimized amplitude and phase values shown in the table 2. The target flip angle was 30°.

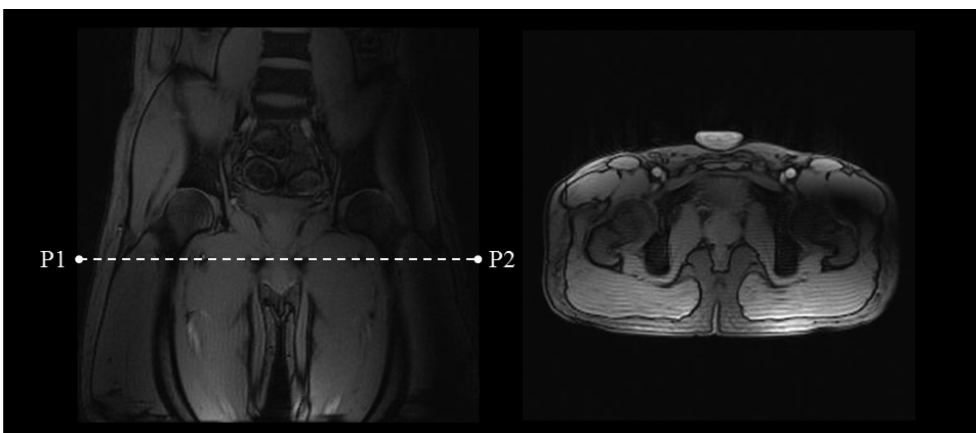


Fig. 7. The human body image with B_1^+ optimized channel driving. The coronal image (left) and axial (right) image were acquired by gradient echo sequence. The P1-P2 line the position of axial slice. The transmission was performed with the proposed 7-channel Tx array and receiving was performed with an 8-channel Rx array combination.

shimming over the male phantom are shown in Fig. 4. The unit used in this figure is a value relative to the maximum value over all B_1^+ values in the axial center slice. The effects of B_1^+ shimming in the simultaneous operation of every channel are shown in Fig. 5. In Fig. 5, the left image is a B_1^+ map before shimming and the right is the B_1^+ map after shimming. In the right image, all Tx channels are modified with optimized amplitudes and phase numbers from the B_1^+ shimming program.

3.3. Human image with B_1^+ mapping and shimming

The flip angle map over the human body was acquired with an AFI sequence and is shown in the Fig. 6. The driving parameters for the individual power amplifiers were set as is shown in Table 2. The targeted flip angle over the patient was 30°, but the generated flip angle differed from expected uniform flip angle. Especially in the back area of the patient, the difference was maximized.

The Tx array was operated in the shimmed circular driving mode with the optimized amplitude and phase values shown in Table 2. The target flip angle was 30°. The acquired human image with a conventional gradient echo sequence is shown in Fig. 7. The coronal image (left) and the axial (right) image were acquired by a gradient echo sequence. The P1-P2 line denotes the position of axial slice. The transmission was performed with the proposed 7-channel Tx array and the receiving was performed with an 8-channel Rx array combination.

In this research, we used commercial equipment. The prostate, which was set as our target ROI, has uniform image quality.

4. Discussion

In the B_1^+ shimming process, we used only simulation data because of the long time required to obtain a B_1^+

field map. Even recent research into shortening field mapping time takes more than 10 minutes for 8- or 16-channels with high resolution. In our future work, we will adapt the method for fast and precise mapping sequences to obtain actual field maps over the patient.

In this research, for the receiving, the multi-channel Rx array coils were used to provide maximally uniform Rx fields in the image. For the human image, 4-channels of the spine array and 4-channel of the flexible array were selected. The Rx sensitivity will be considered through simulation or experimentation. However, in this paper we do not describe the Rx field generated by these Rx array, because we want to focus on the B_1^+ shimming and its clinical usefulness as a preliminary research tool. This will be verified in our subsequent research with more clinical studies.

In this research, we report the preliminary results of an insertional type pTx array having 7-elements placed in the space above the patient table as a transmit coil, in order to obtain a B_1^+ field for the body object using a 3 T MRI system. Through simulations and imaging, we suggested the possible structure of a multi-channel Tx array and showed the utilities of B_1^+ shimming in multi-channel Tx body imaging at 3 T. The insertional pTx coil combined with the array receiving (Rx) coil provided an enhanced homogeneous B_1^+ field in large ROI imaging as a result of B_1^+ shimming over the body-sized phantom. Through this research, we hope to prove the usefulness of the proposed insertional type RF coil combination for 3 T body imaging.

Acknowledgement

This work was supported by a grant of the Korea Health

Technology R&D Project through the Korea Health Industry Development Institute (KHIDI), funded by the Ministry for Health and Welfare, Korea (HI14C1135).

This research was supported by the National Research Foundation of Korea (NRF) Grant funded by Korea Government (MSIP) (no. NRF-2014M3C7033998).

References

- [1] P. A. Bottomley and E. R. Andrew, *Phys. Med. Biol.* **23**, 630 (1978).
- [2] J. T. Vaughan, M. Garwood, C. M. Collins, W. Liu, L. DelaBarre, G. Adriany, P. Andersen, H. Merkle, R. Goebel, M. B. Smith, and K. Ugurbil, *Magn. Reson. Med.* **46**, 24 (2001).
- [3] T. S. Ibrahim, R. Lee, B. A. Baertlein, A. M. Abduljalil, H. Zhu, and P. M. Robitaille, *Magn. Reson. Imaging* **19**, 1339 (2001).
- [4] C. M. Collins, W. Liu, B. J. Swift, and M. B. Smith, *Magn. Reson. Med.* **54**, 1321 (2005).
- [5] P. F. Van de Moortele, C. Akqun, G. Adriany, S. Moeller, J. Ritter, C. M. Collins, M. B. Smith, J. T. Vaughan, and K. Ugurbil, *Magn. Reson. Med.* **54**, 1503 (2005).
- [6] J. Kevin, J. Chang, and I. R. Kamel, *Appl. Radiol.* **39**, 22 (2010).
- [7] G. Adriany, P. F. Van de Moortele, J. Ritter, S. Moeller, E. J. Auerbach, C. Akqun, C. J. Snyder, T. Vaughan, and K. Ugurbil, *Magn. Reson. Med.* **59**, 590 (2008).
- [8] Y. B. Kim and Y. C. Ryu, *Trans. Korean Inst. Electr. Eng.* **63**, 546 (2014).
- [9] Y. C. Ryu and Y. B. Kim, *Trans. Korean Inst. Electr. Eng.* **63**, 404 (2014).
- [10] Parallel RF Transmission: RF Shimming GUI (<http://cai2r.net/resources/software/parallel-rf-transmission-rfshimming-gui>)
- [11] V. L. Yarnykh, *Magn. Reson. Med.* **57**, 192 (2007).